DOI 10.1007/s10946-015-9527-7
Journal of Russian Laser Research, Volume 36, Number 5, September, 2015

EFFECT OF PRELIMINARY HEATING OF A POLYMERIC POLYTETRAFLUOROETHYLENE TARGET ON ITS ABLATION BY A CONTINUOUS CO_2 LASER

E. M. Tolstopyatov,[1] P. N. Grakovich,[1] L. F. Ivanov,[1] S. R. Allayarov,[2,3] Yu. A. Olkhov,[2] and D. A. Dixon[3]*

[1] *V. A. Belyi Metal-Polymer Research Institute of National Academy of Sciences of Belarus Gomel 246050, Belarus*

[2] *Institute of Problems of Chemical Physics of Russian Academy of Sciences Chernogolovka 142432, Moscow Region, Russia*

[3] *Department of Chemistry, University of Alabama Tuscaloosa, AL 35487-0336, USA*

*Corresponding author e-mail: dadixon@as.ua.edu

Abstract

We study experimentally the effect of pre-heating polytetrafluoroethylene (PTFE) on its laser ablation rate from a continuous wave CO_2 laser. The ablation rate and the fraction of fiber formed grow significantly as the initial temperature of the polymeric target increases from 292 to 683 K. The ablation rate obeys two exponential dependences on the temperature with different apparent activation energies for the high-temperature and low-temperature regimes. We find that a crossover temperature of 460 K correlates best with the temperature for sol–gel transformation in the bulk. The faster rates at higher temperature are due to the ability of the reactive species generated in the ablation process to react with more of the system.

Keywords: polytetrafluoroethylene, molecular-topologic structure, laser ablation, continuous CO_2 laser, DSC, TGA, polymeric target.

1. Introduction

Polytetrafluoroethylene (PTFE) is an important polymer for many applications due to its unique properties. It has a high chemical and thermal stability [1] among synthetic polymers, but very low γ-radiation [2] and laser stability [3,4]. If one can understand the mechanism of degradation by radiation of different energies, the range of applications of PTFE could be expanded, for example, for applications in space.

Laser ablation of polymers using pulsed lasers has been reviewed in the literature [5–8]. Radiation from a CO_2 laser operating in continuous mode with a wavelength of 10.6 μm is of interest for use in ablation processes because it is the simplest, most powerful, and most commonly used industrial laser. Earlier works on laser ablation of polymers were focused on thin film polymer coating deposition in vacuum using a CO_2 laser operating in continuous and quasi-pulse modes [5]. Unlike most polymers, PTFE does not produce condensable molecular species during ablation as the product gases consist only of C_2F_4 and

Manuscript submitted by the authors in English on August 6, 2015.

C_3F_6 [9]. There are reports on the thin coating deposition of PTFE with pulsed laser ablation [10–13], but this is only possible when the ablation products contain heavy condensable molecular species.

The molecular–topographical characteristics of PTFE irradiated by a laser at 296 K have been described in [3, 4]. The polymer treated by laser irradiation becomes partly amorphous with the degree of amorphization and other changes depending on the radiation fluence. A decrease in the onset of molecular flow and initial melting temperatures of the crystalline polymorphs, a decrease in the molecular mass, and the disappearance of the crystalline branching points characteristic of the original polymer were observed in the laser-irradiated polymer.

It is likely that the most significant difference between continuous and pulsed irradiation of a solid body lies in the degree of heat transfer from the surface area of radiation absorbance to the total volume. The focus of the present investigation is to estimate the influence of the initial temperature of the polymeric target on ablation of PTFE using a continuous CO_2 laser.

Very few solvents will dissolve PTFE, and its solvent resistance is an asset, although its lack of solubility precludes many of the tradition polymer characterization techniques, such as molecular weight determination by the gas–liquid chromatography. The existing methods of polymer molecular heterogeneity are based on the properties of dilute solution. Such methods allow for the analysis only of soluble polymers. For insoluble polymers such as PTFE, these methods cannot be applied. Thermomechanical spectroscopy (TMS) is a technique for determining the polymer molecular-topographical structure. It is based on the thermomechanical analysis of a polymer and allows complex polymer molecular-topographical testing. We previously used TMS to study the influence of γ [14–16] and laser [3, 4] irradiation on PTFE. In the present work, TMS is used to investigate the molecular-topological characteristics of the PTFE to identify its phase behavior at different temperatures.

2. Experimental

2.1. Materials

Commercial PTFE of F4-type from Konstantinov Kirovo–Chepetsk Chemical Combine (Russia) was used. It is the product of PTFE pressing followed by "calcination."

2.2. Laser Irradiation of the Heated Target of PTFE

The laser irradiation was carried out in a universal vacuum installation VUP-4 [9,17], with a vacuum chamber with a volume of 16 l, which was additionally equipped with a commercial laser of LGN-703 trade mark. The diameter of the laser beam is 8–9 mm, and its power was 28 or 37 W. The light intensity distribution in the laser beam cross section was stable after 20 min of non-ablative operation; at this point, target irradiation was initiated. The laser beam was introduced into the vacuum chamber through a sodium chloride window. Before laser ablation, the vacuum chamber was evacuated to a pressure of 10^{-3} Pa. The chamber is kept under vacuum during ablation. However, the pressure in the working chamber increased to 100–200 Pa due to the intense emission of gaseous products generated by the destruction of PTFE. The time of laser irradiation was 30 s. The mass of the ablated species was determined by weighing of the polymeric target before and after laser irradiation. The average rate of ablation was calculated by dividing the target weight loss by the time of irradiation.

2.3. Thermomechanical Analysis

The molecular–topological structure of the polymer used as target was investigated by TMS [18, 19]. The analysis was carried out by penetration of a quartz hemispherical probe into the polymer. The dynamics of its interaction with a polymer surface has been described in [20]. The symbol notation used in the text are from the literature [3, 4, 18]. For TMS analysis, the polymer sample was placed in the chamber of the standard thermoanalyzer UIP-70M and cooled to 173 K at a rate of 5 deg/min. It was maintained at this temperature for 5 min and then the probe was loaded with a force of 0.5 g. Finally the sample was heated at a rate of 5 deg/min. The accuracy and reproducibility of the TMS method was analyzed previously [21]. The accuracy of the temperature measurements in the thermostatic chamber of the instrument is ±0.05 K. The accuracy of the deformation measurement is ±5 nm. The errors of the molecular mass (MM) and free volume fraction are less than or equal to ±10%. The data were reproducible within the error limits of ±5 to 10%, but in some cases, it can be as large as ±20% due to heterogeneity of the materials and differences in their thermal and stress history.

2.4. Thermal Analysis

The standard synchronous thermal analyzer STA 409C Luxx from the German firm NETZSCH, interfaced with a quadrupole QMS 403C Areolas mass-spectrometer was used for the simultaneous determination of the change in weight (TG) and quantitative measurement of thermal effects (DSC) using a set temperature program. Measurements were performed in an atmosphere of Ar, and aluminum pans were used as crucibles. A thermocouple of S (Pt/Pt-Rh) type was used to measure the temperature. The quadrupole mass-spectrometer is interfaced with a thermoanalyzer by means of a flexible quartz capillary, which can be heated up to 573 K. This prevents the possible condensation of reaction products. The device is able to analyze more than 60 lines due to different mass numbers in the range of $m/e < 300$). The electron impact energy was 70 eV.

3. Results and Discussion

The samples of the polymeric target were heated in the temperature range 293–673 K to investigate the influence of heating on the process of the laser ablation. The samples were in the appropriate phase state at the temperature at the moment of the start of laser irradiation. The phase behavior of the polymer was investigated by the TMS method.

3.1. The Molecular–Topological Structure of the Polytetrafluoroethylene

The thermomechanical curve of PTFE is a characteristic of the semi-block amorphous crystal structure (Fig. 1). In the temperature range from 173 to 289 K, PTFE exists in a semi-crystalline state and expands with temperature at a constant rate (AB line), which is characterized by a coefficient of linear thermal expansion $\alpha_1 = 4.46 \cdot 10^{-5}$ deg^{-1}. In the temperature range from 173 up to 823 K, the largest transition occurred near 298 K. A similar glass transition temperature was reported previously [22]. At $T_g = 289$ K, the polymer exhibits an enhanced segmental mobility and formation of the transition area of thermomechanical curve, as shown by the deformation jumps ΔH_i. This deformation is the result of the decrease in the amorphous form as a consequence of the increasing molecular weight of the polymer homolog [23, 24].

At the temperature T_∞ (point C), the highest molecular inter-bundle homolog transforms to the sol–gel state. In the current sample of PTFE, this state is reached at 523 K. At a higher T_∞ temperature, the amorphous fraction of PTFE transforms into the high elasticity state (straight line D). The polymer expansion, which depends on temperature, is due to an increase in the geometric free volume of the polymer V_f and is characterized by the linear thermal expansion factor $\alpha_2 = 19.53 \cdot 10^{-5}$ deg^{-1}. The criterion of the topological composition of PTFE is the plateau of highly-elastic deformation (curve CD), where the ratio of the expansion rates in this area is $\alpha_2/\alpha_1 < 6$ [25]. The dependence of the quantities α_1, α_2, and V_f with the glass transition temperature T_g has been established in [26] and is given by the following equation:

$$V_f = 3(\alpha_2 - \alpha_1)T_g. \tag{1}$$

The value $V_f = 0.131$ characterizes the amorphous portion of the PTFE as a rigid chain polymer. The pseudo-network structure of the amorphous block is formed from the crystalline fragments of PTFE macromolecules, which function as inter-chain branching elements. Their thermostability is limited by the beginning of the flow temperature of the crystalline fraction. The flow of the crystalline form was characterized by a sharp increase in the rate of deformation (straight line DC$^{\mathrm{I}}$). At 563 K, it has reached equilibrium and can be characterized by the linear thermal coefficient of thermal expansion α_k and the flow of the low melting crystal fraction. The quantitative value is proportional to the total specific expansion deformation H_{cr1}/H_o, where H_o is the height of the sample. At $T > T_m$, the rate of the polymer expansion sharply increases as a result of the increase in polymer volume during melting [17].

At 579 K, fusion of the low-melting crystalline modification ends. The polymer again passes to an area of high elasticity expansion with the rate of expansion equal to α_2. This occurs due to an increase in the free volume in an amorphous form of PTFE (straight line C$^{\mathrm{I}}$D$^{\mathrm{I}}$). At $T'_m = 630$ K, the polymer expansion begins again with the characteristic expansion rate for the fusion of a crystal phase ($\alpha_k^{\mathrm{I}}/\alpha_1 > 6$) (straight line D$^{\mathrm{I}}$). At 713 K, the flow of the intermediate melting crystalline region ends. The deformation process again transfers into the mode of high elasticity with rate of expansion α_2 (C$^{\mathrm{II}}$D$^{\mathrm{II}}$). In this region, the expansion is stable up to 718 K. At this point, the flow of the more refractory crystal modification is observed with an expansion rate α_k^{II}. This is the high-melting crystalline region of PTFE. The values of the weight degree of total crystallinity ($\Sigma\psi = \psi_{\mathrm{cr}} + \psi_{\mathrm{cr}}^{\mathrm{I}} + \psi_{\mathrm{cr}}^{\mathrm{II}}$) is 0.54 (see Table 1), in good agreement with a value for the crystallinity of ∼0.6 for this specific commercial PTFE sample determined by other methods [27, 28].

In the field of flow of the PTFE crystalline phase at 783 K, the first indications of thermomechanical polymer deformations are observed. As in any linear polymer, this is complete at a temperature only a few degrees higher than the temperature of molecular flow (point O). Heating was stopped at 823 K, because at this temperature, there is fast thermal degradation of PTFE as gas is evolved and the polymer weight decreases. Thermogravimetric analysis confirms this observation. As shown on the thermogravimetric curve (Fig. 2, curve 1), an apparent mass loss occurs at temperatures above 814 K. The first evidence for the PTFE mass loss was detected at 623 K but, because the temperature ramping is being carried out slowly, the mass loss is less than 1% at 783 K. This mass loss is probably due to the destruction of impurities which were incorporated during the synthesis of PTFE, and is not related to the thermal destruction of C–C or C–F bonds. At 814 K, the polymer loses about 3% of its weight. On further heating, the rate of the mass loss will accelerate. At 872 K, the polymer is losing 75% of its mass.

Table 1. The Molecular Morphology of PTFE from the TMS Analysis.

Parameter	Value	Parameter	Value
Amorphous region		Intermediate-melting crystalline portion	
T_g, K	289	T'_m, K	630
$\alpha_1 \cdot 10^5$ deg^{-1}	4.46	T_f, K	713
$\alpha_2 \cdot 10^5$ deg^{-1}	19.53	$\bar{M}^{\mathrm{cr1}} \cdot 10^{-3}$	25200
V_f	0.131	$\psi^{\mathrm{I}}_{\mathrm{cr}}$	0.17
$\bar{M}_{g_n} \cdot 10^{-3}$	133.3	High-melting crystalline portion	
$\bar{M}_{g_w} \cdot 10^{-3}$	225.4	T''_m, K	718
K_a	1.69	T_f, K	776
ψ_a	0.46	Δ, K	58
Low-melting crystalline portion		$\bar{M}^{\mathrm{cr2}} \cdot 10^{-3}$	44369
T_m, K	563	$\psi^{\mathrm{II}}_{\mathrm{cr}}$	0.22
T_f, K	579	Values averaged between regions	
$\bar{M}^{\mathrm{cr}} \cdot 10^{-3}$	7.9	$\overline{\overline{M}}_w \cdot 10^{-3}$	14150
ψ_{cr}	0.15	T_f, K	776

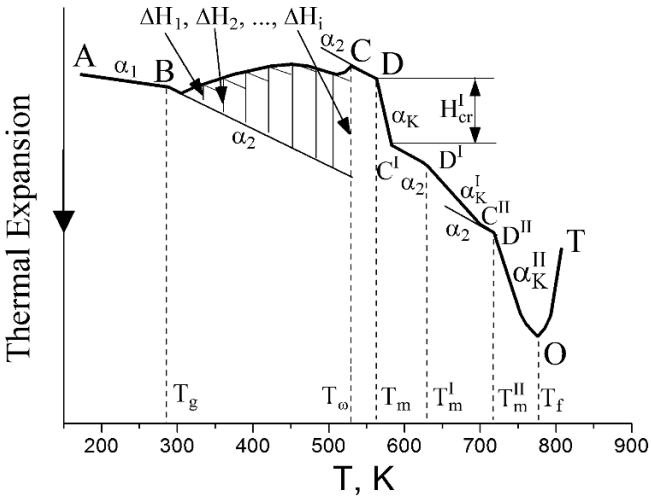

Fig. 1. Thermomechanical curve of PTFE.

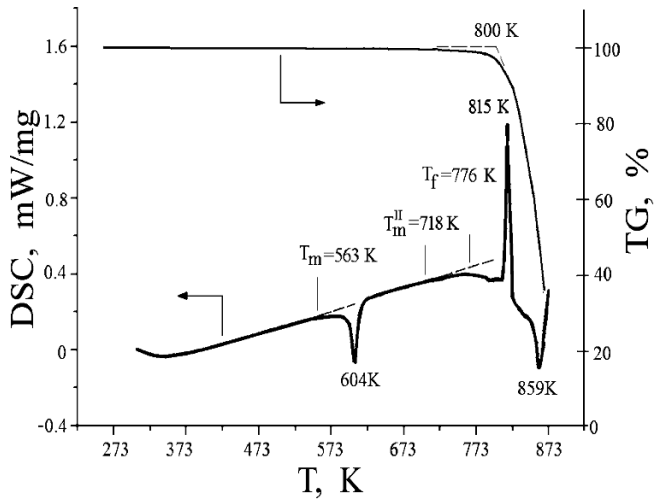

Fig. 2. Thermogravimetric curve 1 and DSC curve 2 of PTFE.

The differential scanning calorimetry (DSC) curve of PTFE is presented in Fig. 2, curve 2. From the DSC curves up to 592.8 K, the PTFE is in an amorphous state. Above this temperature, the endothermic peak of the fusion of the crystal phase is formed at 604.2 K. The enthalpy of melting is 17.6 J/g. These parameters for heating PTFE are in good agreement with the data available in [29]. The heat of fusion determined by the differential scanning calorimeter DSM-2 of the film produced from the same PTFE of mark F4 is 16.5 ± 1.3 J/g [29]. At ∼588 K, the beginning of an endothermic process of fusion of the PTFE with a peak at ∼598 K has been observed in [29].

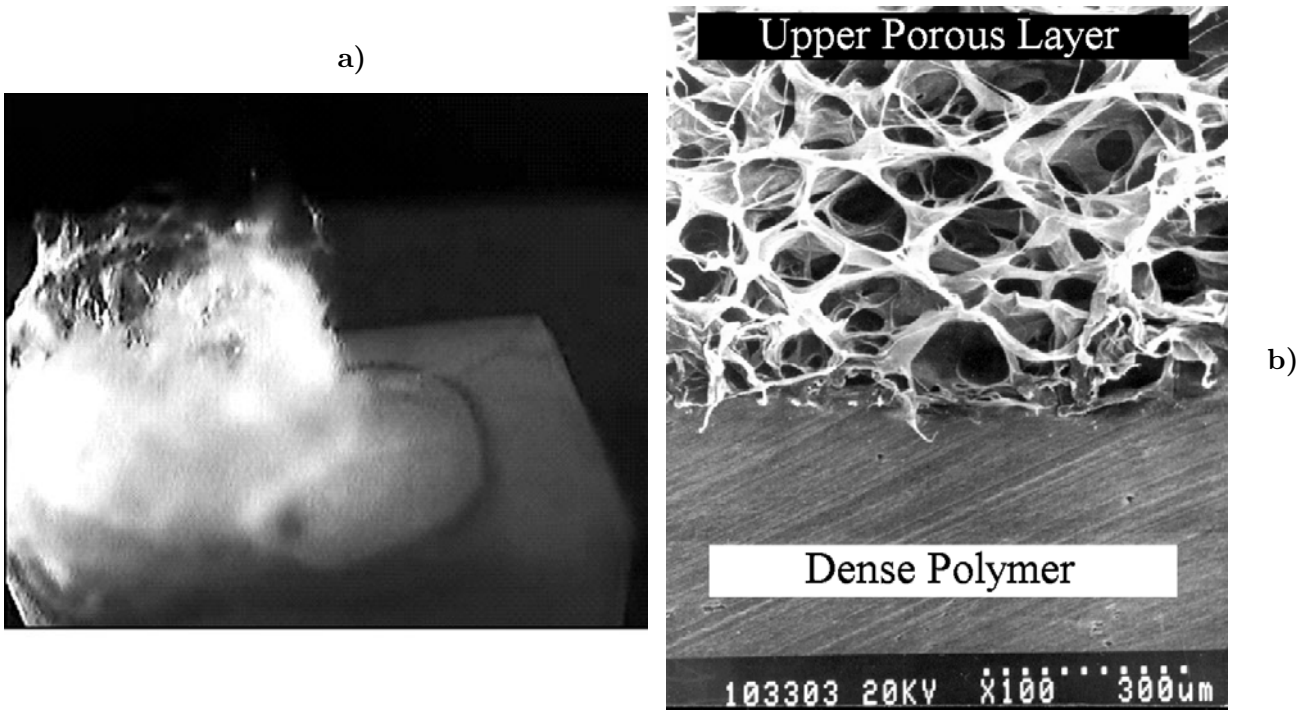

Fig. 3. View of the PTFE target in the vacuum chamber during laser irradiation (a) and the cross section of the surface layer of the ablation crater (b).

The fusion temperature detected in the DSC curve (Fig. 2, curve 2) corresponds approximately to the midpoint between the melting temperatures of the low-melting and intermediate-melting crystals detected in the TMS curve (Fig. 1). In the DSC curve of the PTFE, the exothermic effect occurs only at 815 K with an enthalpy 33.6 J/g. The last process can be interpreted as the temperature of the effective breaking of the covalent bonds in PTFE.

Thus, the existence of the four-block topological structure composed of one amorphous ($T_g = 289$ K) and three crystalline (low-melting ($T_m = 563$ K), an intermediate ($T_m^{\mathrm{I}} = 630$ K), and a high-melting ($T_m^{\mathrm{II}} = 718$ K) polymorphs was revealed in the range of 173 K–800 K by TMS. DSC and TGA analysis of the PTFE show that breaking of covalent bonds and effective thermal degradation of the PTFE happens above 814 K. The results confirm that preheating of the polymer target even up to 700 K does not lead to much destruction of the PTFE macromolecules. Thus, the temperatures used in the present work for heating of the polymeric target from 293 K to 690 K cannot lead to significant destruction of the PTFE macromolecules as they are below 814 K.

3.2. Laser Irradiation of Heated PTFE

The impact of the highly intensity laser radiation on the PTFE target in vacuum is accompanied by the release of gaseous products of degradation and, in some cases, of clusters of the partially destroyed polymer [9,30]. PTFE exhibits an abnormal behavior in this process. After being exposed to continuous CO_2 laser radiation, it degrades at a high rate, and the remaining TFE forms fibrous clusters. A unique feature of PTFE ablation by means of continuous wave CO_2 laser radiation is the release of polymer fibers from the crater (Fig. 3 a) and formation of a fully foamed layer (Fig. 3 b).

Experiments carried out using targets from different manufacturers reach up to 15% of transformation

of the polymer into the fibrous form. The yield of the fiber products depends on the polymer production mode. For example, if the targets were prepared from PTFE powder, the yield of fiber fraction depends on how the powder is pressed and sintered. The sample of PTFE used in the present work gives 13.8% of the yield of the fiber fraction after 30 s of laser ablation for an initial temperature of the polymeric target of 293 K.

To study of the influence of heating of the PTFE target on its laser ablation, temperatures were chosen corresponding to the phase transitions of PTFE as determined by the TMS analysis described above. They include the region of temperature 293–673 K, where the molecular–topological transformation of the structure of the PTFE occurs for both the amorphous region and the crystalline phase. The dependence of the yield of products of the laser ablation of PTFE on the initial temperature of the polymeric target is presented in Figs. 4 and 5 for the yield of gaseous and fibrous products, respectively.

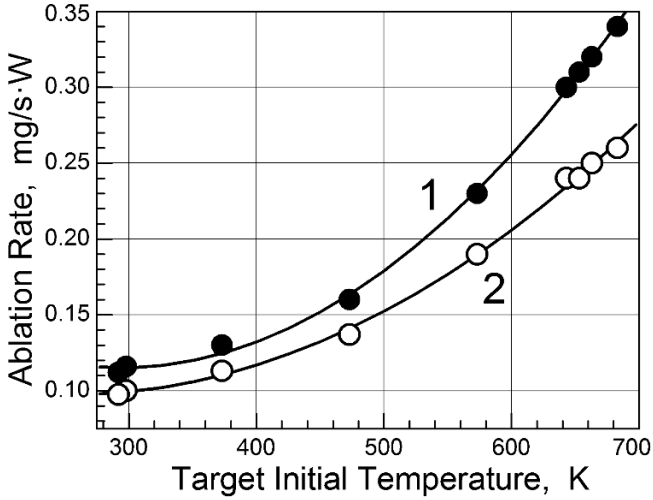

Fig. 4. Dependence of ablation rate on the initial temperature of the target when using the laser beam with power 37 W. The total rate (curve 1) and the rate of emission of gaseous products (curve 2).

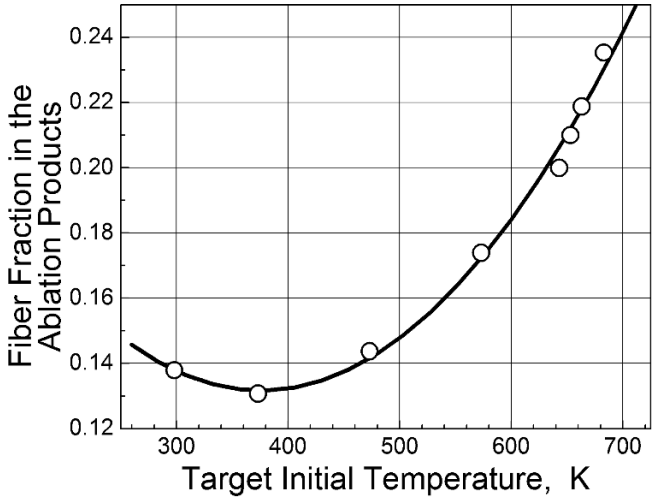

Fig. 5. Dependence of yield of the fibrous products of ablation on initial temperature of the polymeric target from PTFE.

The dependence of the ablation rate on the initial temperature of target (Fig. 4) is explored using a laser with a beam power of 37 W. A similar dependence is observed when using a laser with a power of 28 W. The analysis of the results confirms that the process of ablation will proceed in essentially the same way in the region of 28–37 W of power with an equal mass of ablated products per 1 J of the laser energy.

The rate of ablation increases by a factor of 2.8 when the initial temperature of the target was increased from 293 to 673 K. This can be explained by the decrease in energy required for heating the polymer target up to temperatures of destruction. It could also be the result of phase transitions occurring in the polymer during the preliminary heating of polymeric target. If the latter is true, heating of the target above the polymer melting temperature should be accompanied by a jump in the speed in the curve of ablation rate vs pre-heating temperature. However, such an increase in speed of ablation is not observed experimentally.

Analysis of the curve of the variation of yield of fibrous products on temperature shows that the yield of the fiber fraction increases by a factor of 1.7 in the investigated temperature range (Fig. 5). This can

be explained as an increase in the thickness of the layer involved in the process of thermal destruction of the area of the polymer under the laser beam. At the same time, the transition layer between the compact and fully foamed layer of the crater formed at laser ablation of TFE is very narrow (Fig. 3 b). The intense gas release due to the thermal destruction of the irradiated polymer happens in an interlayer not thicker than 30 μm.

Figure 6 presents the Arrhenius plot of the dependence of the gas emission rate on inverse temperature. The observed dependence can be formally described by two linear functions for the high temperature and low temperature ranges with apparent activation energy 8.4 kJ/mole and 1.7 kJ/mole, respectively. The apparent activation energy term has to be used as the mode of heating cannot to be the main source of energy for polymer destruction or ablation. The crossover point for the high temperature and low temperature lines is 460 K, so at this target temperature there is an apparent change in the kinetics of the polymer ablation. However, this temperature is not a characteristic temperature of a polymer phase transformation as observed by our TMS and DSC investigations. It coincides with the temperature of transformation of the rigid fixed macromolecules into the sol–gel state in the transition area of curve of TMS. The observed threshold temperature of 460 K is below the temperature of melting of PTFE from the DSC measurement (see the endothermic curve in the temperature interval 589–623 K in Fig. 2, curve 2) and below the temperatures of melting of the high, intermediate, and low melting crystalline forms of PTFE (see the TMS curve with initial flow temperatures of 718, 630, and 563 K, respectively, in Fig. 1).

The appearance of the crossover point at 460 K for the dependence of the product yield on the initial temperature of the polymeric target is a result of a change in the reactivity of the polymer with radicals and other active species generated during ablation. It has been established [4, 31] that, at the moment of laser ablation, the reactive species $:CF_2$ and F are formed due to destruction of PTFE macromolecules. The F is generated by breaking a CF bond and the $:CF_2$ is generated as the chain decomposes after a C–F bond in a terminal CF_3 group is broken. The carbene and the atomic radical participate in chemical reactions with PTFE, which lead to the formation of fibrous and gaseous products [4]. Due to these reactions, the polymer has a lower viscosity and its decomposition now differs from that of native PTFE. The increase in the target temperature can increase diffusion of the active species in the polymer volume and the bulk of the modified polymer. The fact that the yield of the fiber fraction in the temperature range 290–460 K does not change suggests that the reactive species are not able to readily leave the ablation site and react further with the bulk of the polymer. The presence of the crossover temperature is undoubtedly not random and indicates the existence of at least two processes influencing the ablation process and mechanism of fiber formation. The first is probably the reactions of the native macromolecules of PTFE, and the second is the reaction with products generated by the first stage.

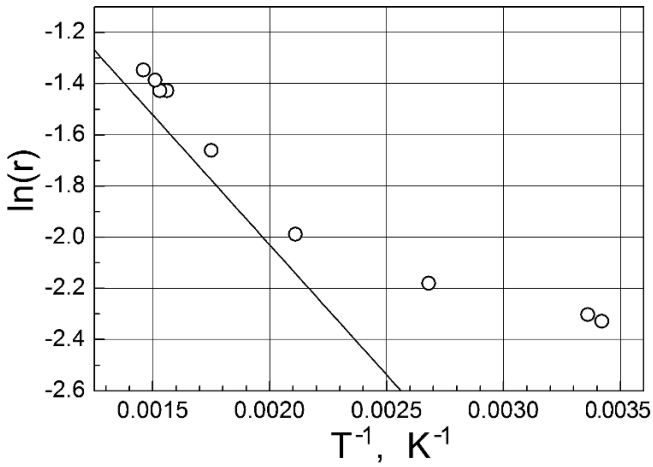

Fig. 6. Dependence of the gas emission rate on preheating temperature of the polymeric target from PTFE during laser ablation.

The views of the process of laser ablation (a) and the cross section of surface layer of the ablation

crater (b) presented in Fig. 3 confirm that the ablation of PTFE happens with the formation of gaseous and fibrous products. The fiber fraction of the PTFE after laser ablation has a lower molecular mass as compared to the original polymer [4]. The difference in molecular structure of the fiber fraction and the original polymer is demonstrated by the results from the secondary ablation of the fibers as this is accompanied by emission of heavy molecular fragments capable of condensing on solid surfaces in the form of a coating.

4. Summary

The yield of products of the laser ablation depends on the initial temperature of the polymeric target from PTFE. The rate of laser ablation of PTFE obeys two different exponential dependences on the temperature of heating of the polymeric target with apparent activation energies for the high-temperature regime of 8.4 kJ/mole and for the low-temperature regime of 1.7 kJ/mole. The crossover of the high temperature and low temperature linear fits on the Arrhenius plot is 460 K. This temperature is not a characteristic temperature of the polymer phase transformations in PTFE. It coincides with the temperature of transformation of the rigid fixed macromolecules into the sol–gel state in the transition area of the TMS curve. The observed crossover temperature of 460 K is below the melting temperature of PTFE registered by DSC and of the melting temperatures of the high, intermediate, and low melting crystalline forms of PTFE as determined by TMS. The appearance of the crossover temperature of 460 K is a result of a change in the ability of the reactive species generated by laser ablation to react further with the bulk of the polymer at higher temperatures than at lower temperatures due to a change in their diffusivity.

Acknowledgments

The authors thank the Cooperative Grants Program of the U.S. Civilian Research and Development Foundation for financial support under Grant No. RUC1-7093-MO-13. D.A.D. thanks the Robert Ramsay fund of The University of Alabama for partial support.

References

1. J. Scheirs, *Modern Fluoropolymers: High Performance Polymers for Diverse Applications*, John Wiley & Son Inc., New York (1997).
2. V. S. Ivanov, *Radiation Chemistry of Polymers*, VSP, Leiden (1992).
3. L. F. Ivanov, Yu. A. Olkhov, S. R. Allayarov, et al., *High Energy Chem.*, **48**, 117 (2014).
4. Yu. A. Olkhov, S. R. Allayarov, E. M. Tolstopyatov, et al., *High Energy Chem.*, **44**, 63 (2010).
5. D. B. Chrisey, A. Pique, R. A. McGill, et al., *Chem. Rev.*, **103**, 553 (2003).
6. T. Lippert, in: A. Miotello and P. M. Ossi (Eds.), *Laser-Surface Interactions for New Materials Production Tailoring Structure and Properties*, Springer Series in Material Chemistry, Springer, Berlin (2009), Vol. 130, Ch. 7, p. 141.
7. L. Urech and T. Lippert, in: N. S. Allen (ed), *Photochemistry and Photophysics of Polymer Materials*, John Wiley & Son Inc., New York (2010), Ch. 14, p. 541.
8. M. Lorenz and M. S. Ramachandra Rao, *J. Phys. D: Appl. Phys.*, **47**, 030301 (2014).

9. E. M. Tolstopyatov, L. F. Ivanov, P. N. Grakovich, and A. M. Krasovsky, in: C. R. Phipps (Ed.), *High-Power Laser Ablation*, *Proc. SPIE*, **3343**, 1010 (1998).
10. Y. Ueno, T. Fujii, and F. Kannari, *Appl. Phys. Lett.*, **65**, 1370 (1994).
11. W. Jiang, M. G. Norton, L. Tsung, and J. T. Dickinson, *J. Mater. Res.*, **10**, 1038 (1995).
12. M. G. Norton, W. Jiang, J. T. Dickinson, and K. W. Hipps, *Appl. Surf. Sci.*, **96-98**, 617 (1996).
13. R. Schwodiauer, S. Bauer-Gogonea, S. Bauer, et al., *Appl. Phys. Lett.*, **73**, 2941 (1998).
14. Yu. A. Olkhov, S. R. Allayarov, and D. A. Dixon, *High Energy Chem.*, **48**, 152 (2014).
15. S. R. Allayarov, Yu. A. Olkhov, D. A. Dixon, and D. E. Nikles, *High Energy Chem.*, **48**, 104 (2014).
16. Yu. A. Olkhov, S. R. Allayarov, and D. A. Dixon, *High Energy Chem.*, **46**, 369 (2012).
17. L. Mandelkern, *Crystallization of Polymers*, McGraw-Hill, New York (1964).
18. Yu. A. Olkhov, S. R. Allayarov, T. A. Konovalova, et al., *J. Appl. Polym. Sci.*, **108**, 2085 (2008).
19. Yu. A. Olkhov and E. R. Badamshina, *Int. J. Polym. Mat.*, **19**, 117 (1993).
20. I. I. Vorovich and Iu. A. Ustinov, *J. Appl. Math. Mech.*, **23**, 445 (1959).
21. B. Jurkowski and Yu. A. Olkhov, *Thermocchim. Acta*, **414**, 243 (2004).
22. E. L. Gal'perin and D. J. Tsvankin, *Vysokomol. Soedin.*, **18A**, 2691 (1976).
23. Y. A. Olkhov and V. I. Irzhak, *Vysokomol. Soedin.*, **40B**, 1706 (1998).
24. Y. A. Olkhov, S. M. Baturin, and V. I. Irzhak, *Vysokomol. Soedin.*, **38A**, 849 (1996).
25. J. D. Ferry, *High Elastic Properties of Polymers*, John Wiley & Sons, New York (1980).
26. R. Simha and R. F. Boyer, *J. Chem. Phys.*, **37**, 1003 (1962).
27. J. A. Panshin, S. G. Malkevich, and S. Dunaevskaja, *Fluoroplastics* [in Russian], Khimiya, Leningrad (1978).
28. M. A. Bruk, A. V. Spirin, S. A. Khatipov, and N. V. Kozlova, *High Energy Chem.*, **38**, 239 (2004).
29. A. A. Koptelov and O. F. Shlenskii, *High Energy Chem.*, **36**, 217 (2002).
30. E. M. Tolstopyatov, *J. Phys. D: Appl. Phys.*, **38**, 1993 (2005).
31. J. Pola, D. Tomanová, P. Schneider, et al., *J. Fluor. Chem.*, **50**, 309 (1993).